Why is the F_2 bond so weak? A bond energy decomposition analysis

Linnea E. Forslund and Nikolas Kaltsoyannis*

Department of Chemistry, University College London, 20 Gordon Street, London WC1H 0AJ, UK. E-mail: n.kaltsoyannis@ucl.ac.uk http://www.chem.ucl.ac.uk/people/nkalt/index.html

Received (in London, UK) 18th February 2003, Accepted 4th April 2003
First published as an Advance Article on the web 3rd June 2003

The bond energies of F_2, Cl_2, Br_2 and I_2 have been studied computationally using gradient-corrected, relativistic density functional theory with large all-electron basis sets. The bond energies of all four compounds have been broken down into electrostatic, Pauli (exchange) and orbital terms at the equilibrium internuclear separation and as a function of r(X–X) using the Ziegler–Rauk energy decomposition scheme. The comparative weakness of the F_2 bond is traced to the electrostatic energy, which is considerably smaller than would be expected on extrapolation of the trend in the $I_2 \rightarrow Cl_2$ data. The small electrostatic term is itself a result of the F–F bond being *c.* 0.1 Å longer than might be expected, due to the large gradient in the Pauli repulsion around the equilibrium internuclear separation. The weakness of the F_2 bond is therefore a combination of quantum mechanical (Pauli) and classical (electrostatic) factors. The present conclusions are placed throughout in the context of previous research.

Introduction

It is well known that the bond dissociation energy of F_2 is significantly smaller than would be expected from extrapolation of the I_2, Br_2 and Cl_2 values (I_2: 35.6 kcal mol^{-1}, Br_2: 45.4, Cl_2: 57.2, F_2: 36.9).[1] Indeed, the F–F bond is one of the weakest of all covalent bonds. This anomaly has prompted numerous studies going back to the middle of the last century, and includes contributions from such distinguished chemists as Pitzer, Pauling, Coulson and Mulliken.

In this paper we report the results of our own investigation into the bond energy of the diatomic halogens F_2, Cl_2, Br_2 and I_2. We have used modern density functional theory to probe the electronic structure of the molecules as a function of internuclear separation, and have broken down the bond energy into chemically useful components using the energy decomposition scheme developed by Ziegler and Rauk.[2,3] Our aims were twofold; to see how the previous explanations of the weakness of the F_2 bond stand up to this energy decomposition analysis and, of course, to answer the title question.

Following a description of our methodology, we present a brief overview of some of the key previous work on the problem. We then present our own results, and place them in the context of the previous research. Finally we draw our study to a close by summarising our explanation for the weakness of the F_2 bond.

Computational and theoretical details

A. General

The majority of the calculations were performed with the Amsterdam Density Functional (ADF) program suite, versions 2000 and 2002.[4–8] The basis sets were varied as discussed in the main text, but all results, unless otherwise stated, refer to calculations performed with all-electron, uncontracted, quadruple-zeta Slater-type basis sets, supplemented with four polarisation functions. Scalar relativistic corrections[9] were included *via* the ZORA method.[10,11] Spin-orbit corrections were also included, both on the closed shell X_2 molecules and on their open shell atomic fragments. As with the basis sets, the form of the density functional was varied considerably but, unless otherwise stated, all results refer to calculations performed using pure Slater exchange ($\alpha = 2/3$) for the local density approximation, with gradient corrections due to Perdew and Wang (exchange)[12] and Perdew, Burke and Ernzerhof (correlation).[13] The ADF numerical integration parameter was set to 10 in all calculations, and the energy gradient convergence criterion was set to 5×10^{-5} au Å^{-1} in all geometry optimisations.

In order to compare the results from ADF with other DFT calculations, and with *ab initio* methods, a number of calculations have been done using the Gaussian 98 suite of programs.[14] These calculations employed the 6-311+G(df) basis set.

B. Energy decomposition scheme

ADF defines the molecular bonding energy as the energy difference between the molecular fragments in their final positions and at infinite separation. These molecular fragments may be individual atoms or groups of atoms, though in the present study, of course, only atomic fragments are considered (for a discussion of the use of fragments within ADF, please see ref. 15). These fragments are placed at their positions within the molecule. At this point there is an electrostatic interaction between them, comprising the nucleus/nucleus, nucleus/electron and electron/electron Coulombic interactions. This electrostatic interaction E^{el} is computed from the unperturbed and superimposed charge densities of the separate fragments. Next it is ensured that the overall molecular wavefunction satisfies the Pauli principle. This is done by requiring that the one-electron orbitals of the combined fragments form a correct single-determinantal wavefunction. It is extremely unlikely, however, that this will be the case for the fragment orbitals when the fragments are simply placed at their positions within the molecule because the orbitals on the different fragments will not be orthogonal to one another. Thus the next step is to orthogonalise the occupied fragment orbitals to obtain a correct single-determinantal, antisymmetrised molecular wavefunction. This will result in a change in the molecular charge density, and the accompanying energy change is known as the Pauli, or exchange, repulsion E^{Pauli}. The final part of the process is to allow the fragment orbitals to relax to self-consistency. This interaction energy between the orbitals of the various fragments is defined as the electronic (or orbital, E^{orbital}) interaction within ADF, and is computed using the transition state procedure first developed by Ziegler and Rauk.[2,3]

Some previous explanations for the weakness of the F_2 bond

1. In 1955, Pitzer suggested that attractive dispersion forces might significantly contribute to the bond energy in the X_2 family.[16] Using the London formula he calculated that the London term accounts for a non-trivial fraction (*c.* 35%) of the X_2 bond energy for Cl_2, Br_2 and I_2, but makes only a small (*c.* 10%) contribution to the F_2 bond energy. Subtraction of the London term from the total bond energy removes much of the F_2 anomaly.

Several years later, Caldow and Coulson revisited this idea, but came to a different conclusion.[17] They found, on the basis of different polarisabilities and ionization energies from those used by Pitzer, that the dispersion effect is much less significant, and cannot be the source of the anomalous bond energy of F_2.

2. Also in 1955, Mulliken invoked hybridization to explain why Cl_2 has a stronger bond than F_2.[18] Specifically 'the greater strength of the "single" bond in Cl_2 can be understood as a consequence of pronounced partial multiple bond character made possible by d hybridization'. Thus F_2 is not anomalously weak, but Cl_2 anomalously strong.

3. Pauling also suggested that hybridization is important, but in a different way from Mulliken.[19] He argued that the weak F_2 bond arises from destabilizing interactions between unshared electron pairs on the separate F atoms. This effect is reduced in the heavier X_2 due to d hybridization.

4. After suggesting that Pitzer's dispersion argument was flawed, Caldow and Coulson then traced the weak F_2 bond to an anomalously low value of the Coulomb energy.[17] More specifically, they noted that all three contributors to this energy (nucleus/nucleus and electron/electron repulsion, and nucleus/electron attraction) are anomalous when compared with data for Cl_2, Br_2 and I_2. They also noted that 'since all three [contributions to the Coulomb energy] are closely dependent upon the internuclear distance r, it is this quantity which is anomalous'.

5. Twenty years later, Jolly and Eyermann used photoelectron spectroscopic data to calculate localized orbital ionization potentials (LOIPs) of seven molecules, including the $F_2 \rightarrow I_2$ series.[20] These LOIPs are the energies that atomic orbitals (in molecules) would have if they were non-bonding. Comparison of these data with the ionization energies of the valence π and π^* molecular orbitals (MOs) in the X_2 series led these workers to conclude that the weakness of the F_2 bond is due, at least in part, to lone pair/lone pair repulsions between the two F atoms. Within experimental error, there is no such effect in the heavier X_2.

The lone pair/lone pair repulsion argument of Jolly, Pauling and, implicitly, Caldow and Coulson, is the one favoured by modern textbooks of inorganic chemistry.[21,22] Nevertheless, the range of other explanations suggests that this is not a straightforward issue, and we were keen to undertake our own analysis.

Results and discussion

A. Determining the optimal computational parameters

Prior to applying the energy decomposition scheme, we performed many trial calculations to establish the computational parameters (basis set, form of the density functional *etc.*) which best reproduced the experimental bond energies of the X_2 family. Some of the results of these calculations are collected in Table 1 [given as bond dissociation energies (or atomization energies)], together with a selection of *ab initio* and hybrid DFT data obtained by us and other workers.

Turning first to the *ab initio* data, it is clear that the Hartree–Fock approach does a very poor job of reproducing experiment, particularly for F_2, which is calculated to be metastable at this level. Indeed, the failure of the HF approach to give a realistic potential curve for F_2 has been known for more than 40 years, and consequently F_2 has been used as a testing ground for a variety of post-HF methods. In their 2001 contribution, Pittner *et al.*[23] give a summary of many of the previous *ab initio* calculations on F_2, and the reader is directed to this paper for more details. The principal conclusions from these studies are that good agreement between theory and experiment for D_0 for F_2 can be obtained only when i) a large basis set (including f functions) is used ii) at least a six-reference wavefunction is used and iii) dynamic electron correlation is

Table 1 Bond dissociation energies (kcal mol^{-1}) for the diatomic halogen molecules. Unless otherwise indicated, all data have been calculated in the present study. No zero point energies (ZPE) are included unless stated

Method	Basis set	F_2	Cl_2	Br_2	I_2
Experimental[1] D_0		36.9	57.2	45.4	35.6
Ab initio[a]					
HF[32]	cc-pVQZ	−27.3			
HF	6-311+G(df)	−39.1	13.7	14.8	
MP2	6-311+G(df)	35.6	50.3	48.0	
G2(MP2,SVP)[33]	see ref. 33	36.5	58.2		
G2(MP2,SVP)[34]	see ref. 34			43.5	
CCSD(T)[35]	cc-pVQZ	36.7			
CCSD(T)[36]	cc-pVQZ		56.0		
CCSD(T)	6-311+G(df)	27.8	48.5	45.9	
CASSCF + 1 + 2[32]	cc-pVQZ	34.0			
MR-BW-CCSD[23]	cc-pVQZ	31.6			
classical VB[37]	6-31G(d)	28.6			
DFT					
X-only/PW91x/ PBEc/ZORA	DZ (STO)	38.1	33.7	33.3	28.7
X-only/PW91x/ PBEc/ZORA	TZP (STO)	53.3	56.4	47.7	36.3
X-only/PW91x/ PBEc/ZORA	TZ2P (STO)	55.6	59.9	51.9	44.9
X-only/PW91x/ PBEc/ZORA	QZ4P (STO)	56.6	60.3	51.3	44.8
X-only/PW91x/ PBEc/ZORA/ spin-orbit	QZ4P (STO)	55.7	58.4	44.4	32.3
X-only/PW91x/ PBEc/ZORA/ spin-orbit/ZPE	QZ4P (STO)	54.3	57.7	44.0	32.0
VWN/PW91x/ PBEc/ZORA	QZ4P (STO)	66.9	70.7	59.3	53.4
VWN/BLYP/ZORA	QZ4P (STO)	61.6	61.4	51.9	44.8
PBE (local part only)[25]	TZ2P (GTO)	78.2	82.9		
PBE[25]	TZ2P (GTO)	53.4	65.1		
Meta-GGA[25]	TZ2P (GTO)	43.2	59.4		
BLYP[26]	6-311G(d)	49.8			
BLYP[34]	6-311+G(3df)// MP2(fu)/ 6-31G(d)			43.8	
Hybrid DFT					
B3LYP	6-311+G(d)	31.7	49.2	47.8	
B3LYP[38]	TZ2P (GTO)	35.0	51.9		
B3LYP[34]	6-311+G(3df)// MP2(fu)/ 6-31G(d)			41.4	

[a] For a more comprehensive list of previous *ab initio* data, the reader is directed to ref. 23.

properly accounted for. Such conclusions may lead the reader to assume that single reference techniques such as MP2 and standard coupled cluster theory do a poor job of calculating D_0 for F_2, but the data in Table 1 suggest otherwise. Our MP2 value is in good agreement with experiment, and the CCSD(T) approach also does quite well, with a marked improvement with increasing basis set quality. The G2,MP2 method performs excellently. Nevertheless, Pittner *et al.* note that, even though single reference *ab initio* techniques can reproduce D_0 for F_2 very well, they usually give potential curves which start to deviate from a realistic potential curve deduced from experiment at about 2.3 Å, and that multi-reference methods hold more promise for the accurate determination of the full potential curve. To this end, they are developing methods based on multi-reference coupled cluster theory.

Some of our DFT results are shown below the *ab initio* data in Table 1. Interestingly, the lowest quality basis set—double zeta—does well for F_2 but very poorly for the heavier halogens. Moving to TZP and beyond leads to a marked deterioration in the F_2 bond energy, but a significant improvement in the values for the heavier halogens. There is comparatively little difference between the TZ2P and QZ4P data. As expected, the inclusion of spin-orbit coupling has an increasingly significant effect as the halogen becomes heavier.

We have carried out many ADF calculations in which the effect of changing the form of the density functional has been studied. The results are too numerous to fully include in Table 1, but may be summarized as follows:

1. The form of the local density approximation (LDA) has been varied from pure Slater exchange ($\alpha = 2/3$) to the parameterization of Vosko, Wilk and Nusair (VWN),[24] which also includes the effects of electron correlation to some extent. For a given basis set we found that moving from exchange-only to VWN increased the bond dissociation energy by *c.* 10 kcal mol^{-1}, generally taking the values further from experiment (compare the X-only/PW91x/PBEc/ZORA data in Table 1 with those from the VWN/PW91x/PBEc/ZORA approach). We therefore chose the exchange-only form of the LDA.

2. ADF supports a wide variety of exchange and correlation gradient corrections, and we have examined the effect, for a given basis set and LDA form, of varying the form of the GGA (generalized gradient approximation). No one combination of exchange and correlation gradient corrections produced results that were uniformly good for all four X_2 molecules. As with the basis sets, most GGA combinations led to improvements for some X_2 and worse agreement for others. On balance, we have chosen the PW91x/PBEc combination for our studies. Table 1 shows that this combination does well for Cl_2 and Br_2, and gives satisfactory agreement with experiment for I_2. The F_2 value is not good, which is discussed further below. The bond lengths and vibrational frequencies calculated with this method are given in Table 2.

Table 1 shows that other workers have also found that pure DFT methods do a poor job of calculating the bond dissociation energy in F_2. The local part of the PBE functional[25] differs by more than 40 kcal mol^{-1} from experiment, although the inclusion of gradient corrections *via* the PBE approach brings this value down significantly, such that it is close to our gradient corrected value. The use of a meta-GGA further improves both the F_2 and Cl_2 values.† The gradient corrected BLYP value is *c.* 14 kcal mol^{-1} away from experiment.[26]

Table 2 Comparison of experimental and calculated bond lengths and vibrational wavenumbers for the X_2 series

	F_2	Cl_2	Br_2	I_2
Bond lengths/Å				
Experiment[1]	1.41	1.99	2.28	2.67
Calculated	1.43	2.04	2.34	2.73
Vibrational wavenumbers/cm^{-1}				
Experiment[1]	917	560	325	215
Calculated	958	511	299	200

The rather disappointing ability of pure DFT methods to calculate the bond energy of F_2—particularly the failings of the LDA—has been noted before.[27] It is argued that the LDA does poorly when confronted with overlapping lone pairs, as it overestimates the exchange stabilisation resulting from such orbital interactions, and hence the bond energy. The problem is only partially remedied by the inclusion of gradient corrected exchange functionals.

The final methodology given in Table 1 is the hybrid DFT B3LYP approach. This method clearly performs better for F_2 than pure DFT, and comparably for Cl_2 and Br_2.

One of the primary motivations behind our study is to apply the Ziegler–Rauk energy decomposition scheme. We are therefore restricted to the pure DFT approach of ADF, and it is unfortunate that such a methodology does not do a better job at calculating the bond energy of F_2. Nevertheless, the key qualitative features of the experimental data—that F_2 has a weaker bond than Cl_2 and a much weaker bond than would be expected on the basis of the I_2, Br_2 and Cl_2 data—are reproduced by our calculations, and we were hopeful that our study would indeed uncover differences between F_2 and its heavier congeners.

B. Population analysis

We saw earlier how some of the previous explanations for the weakness of the F_2 bond focused on hybridisation effects, specifically *via* the admixture of d character into the valence MOs. Table 3 presents the Mulliken population analysis data for the valence π_g, π_u and σ_g MOs of the X_2 series, from which it can be seen that the π MOs are almost entirely composed of the valence p atomic orbitals (AOs) of the halogen atoms. The largest d contribution is only 2.5% (Cl_2 π_u). The σ_g MOs are slightly less p-based, but still have a minimum of 91% p_z character (Cl_2). Furthermore, the remaining contribution to the σ_g levels is primarily valence s, not d.

Given the data in Table 3, it is difficult to make a strong case for hybridisation effects contributing significantly to the bond energy of the X_2 family. This is particularly true for d hybridisation, in agreement with the results of previous studies suggesting a very limited role for main group d functions in, for example, π backbonding in transition metal phosphine complexes,[28] and the bonding in hypercoordinate main group molecules.[29,30]

C. Energy decomposition analysis

The bond energy of all four X_2 has been broken down into its electrostatic (E^{el}), Pauli (E^{Pauli}) and orbital (E^{orbital}) contributions at the equilibrium internuclear separation. These data are shown in Fig. 1. Note that the energy data reported here are taken from our scalar relativistic calculations, as spin-orbit

Table 3 Mulliken population analysis data for the composition (%) of the valence π_g, π_u and σ_g molecular orbitals of the X_2 series (minimum contribution 1%)

MO	F_2	Cl_2	Br_2	I_2
π_g	99.9 p	98.9 p, 2.1 d	99.2 p, 1.7 d	99.6 p, 1.5 d
π_u	99.4 p	97.5 p, 2.5 d	98.2 p, 1.8 d	97.6 p, 1.8 d
σ_g	93.0 p, 6.5 s	91.4 p, 8.0 s, 1.2 d	94.9 p, 4.7 s	94.6 p, 4.4 s

---

† We have not employed meta-GGAs in our calculations as they are only available in single point calculations in ADF.

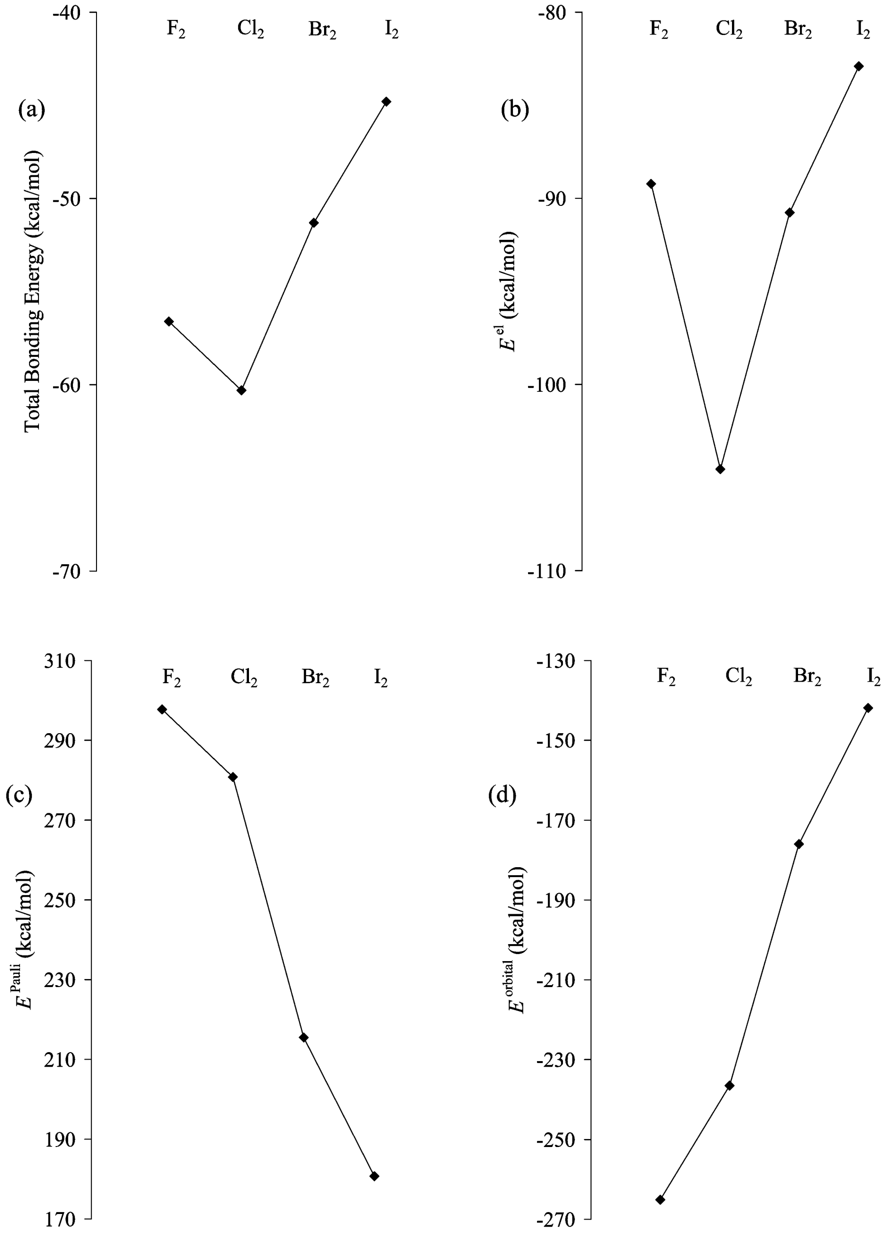

Fig. 1 Bond energy (kcal mol^{-1}) decomposition for F_2, Cl_2, Br_2 and I_2 at equilibrium internuclear separation: (a) total bond energy (b) electrostatic energy (c) Pauli repulsion (d) orbital interaction energy.

coupled open-shell atoms cannot be used as fragments in ADF molecular calculations.

As expected, the electrostatic and orbital terms are both negative. By contrast, E^{Pauli} is positive in all cases, and the total bond energy is clearly a competition between the stabilising E^{el} and $E^{orbital}$ terms and the destabilising exchange repulsion. For the Pauli and orbital terms, there is an approximately linear trend from $I_2 \rightarrow F_2$. The sum of E^{Pauli} and $E^{orbital}$ for each X_2 is plotted on Fig. 2, relative to an arbitrary value of 0 kcal mol^{-1} at I_2. The change in ($E^{Pauli} + E^{orbital}$) from $I_2 \rightarrow F_2$ is non-uniform, as I_2 and Br_2 differ by only 0.7 kcal mol^{-1}, with Cl_2 and F_2 both *c.* 5 kcal mol^{-1} from the I_2 and Br_2 values, in different directions.

The total bonding energy and electrostatic energy for each X_2 are also plotted on Fig. 2, again with reference to an arbitrary value of 0 kcal mol^{-1} at I_2. The trend in both the total bonding energy and E^{el} from $I_2 \rightarrow Cl_2$ is clearer than for the ($E^{Pauli} + E^{orbital}$) data, with a steady increase (more negative) with decreasing atomic number. Clearly, the value of E^{el} for F_2 is significantly less negative than

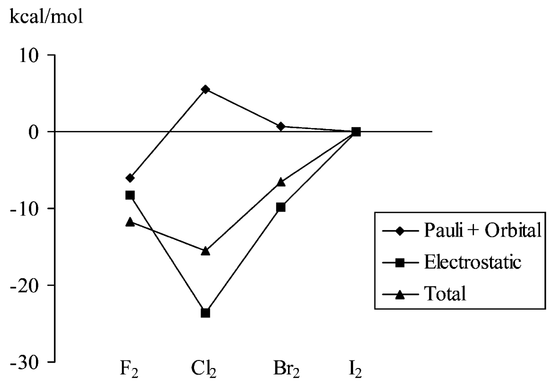

Fig. 2 Total bonding energy, electrostatic energy and (Pauli + orbital) energy (kcal mol^{-1}) for F_2, Cl_2, Br_2 and I_2 at equilibrium internuclear separation, relative to an arbitrary value of 0 kcal mol^{-1} at I_2.

would be expected on extrapolation of the $I_2 \rightarrow Cl_2$ trend. Indeed, such an extrapolation suggests a value of *c.* −120 kcal mol^{-1} for F_2, in comparison with the actual value of −89.2 kcal mol^{-1} [Fig. 1(b)]. We therefore suggest that the reduction in the bond energy from Cl_2 to F_2 is a consequence of the reduced electrostatic contribution in the latter. This opposes (and overcomes) the change in $(E^{Pauli} + E^{orbital})$ from $Cl_2 \rightarrow F_2$.

As discussed above, Caldow and Coulson suggested some 40 years ago that the weakness of the F_2 bond lies in its anomalous electrostatic energy,[17] and our calculations clearly support this conclusion. Caldow and Coulson also noted that all three contributions to E^{el} at r_{eqm} are anomalous for F_2. Unfortunately we are unaware of any way to extract the individual components of E^{el} from the ADF code, and cannot therefore fully test Caldow and Coulson's assertion. However, it is not inappropriate to speculate on the cause of the small E^{el} term for F_2. It is well known from electrostatics theory that the repulsion between two like charge clouds is reduced when the clouds interpenetrate.[31] It may therefore be that the interpenetration of the charge clouds associated with the two separate F atoms is less than is the case for Cl_2, Br_2 and I_2. This will lead to greater electron/electron repulsion in F_2, and an overall reduction in E^{el}.

Caldow and Coulson also noted that the dependence of E^{el} upon bond length suggests that r_{eqm} for F_2 is anomalous. To probe this, we have calculated O_2, S_2 and Se_2 using an identical method to that employed for the X_2 series. The equilibrium bond lengths and the values of E^{el} at those bond lengths are given in Table 4 for F_2, Cl_2, Br_2, O_2, S_2 and Se_2. If we compare the equilibrium bond length of diatomics from the same period, we see that the formally singly bonded Cl_2 and Br_2 have r_{eqm} 0.1 Å and 0.09 Å respectively longer than their group 16 counterparts. By contrast, r(F–F) is 0.19 Å longer than the bond in O_2. Furthermore, E^{el} for O_2 at r_{eqm} is significantly more negative than that for both Se_2 and S_2, by contrast to the marked reduction from Cl_2 to F_2.

These data suggest that the small E^{el} value in F_2 is indeed a consequence of the long r(F–F). To probe this further, we recalculated F_2 with a bond length of 1.34 Å, the value expected upon extrapolation of the differences between Se_2 and Br_2, and S_2 and Cl_2. The energy decomposition data for F_2 at r(F–F) = 1.43 Å and 1.34 Å are given in Table 5, from which it may be seen that compression of the F–F bond produces a marked increase (negatively) in E^{el}. Indeed, if the F–F bond were 1.34 Å long, the trend to more negative E^{el} from I_2 to Cl_2 [Fig. 1(b)] would be continued by F_2. Although we cannot say for certain, the increase in E^{el} from r(F–F) = 1.43 Å to r(F–F) = 1.34 Å fits with our suggestion that electron/electron repulsion is the cause of the low E^{el} value at 1.43 Å. As the bond is compressed, the F charge clouds interpenetrate more and the electron/electron repulsion is reduced.

The obvious question, then, is why is the F–F bond so long? We can make progress by examining Table 5 and Fig. 3, which plots the terms in the energy decomposition analysis for F_2 as a function of internuclear separation. Fig. 3 shows that as the bond length is reduced, E^{el} and $E^{orbital}$ become increasingly favourable, while E^{Pauli} works in the opposite direction. Table 5 shows that E^{Pauli} outweighs $(E^{el} + E^{orbital})$ as the bond is shortened from r_{eqm}. Indeed, it is the Pauli repulsion (specifically its kinetic part) which is responsible in general for the inner repulsive wall in potential wells.[31] As Fig. 3 illustrates, E^{el} only becomes unfavourable at very short internuclear distances, as the nucleus/nucleus repulsion begins to dominate.

Table 4 Equilibrium bond lengths (Å) and electrostatic energies E^{el} (kcal mol^{-1}) for the first three diatomic molecules of groups 16 and 17

	F_2	Cl_2	Br_2	O_2	S_2	Se_2
r_{eqm}	1.43	2.04	2.34	1.24	1.94	2.23
E^{el}	−89.2	−104.6	−90.8	−216.0	−165.2	−138.8

Table 5 Electrostatic (E^{el}), Pauli (E^{Pauli}) and orbital ($E^{orbital}$) contributions (kcal mol^{-1}) to the total molecular bonding energy of F_2 at r(F–F) = 1.43 Å and r(F–F) = 1.34 Å

	E^{el}	E^{Pauli}	$E^{orbital}$
r(F–F) = 1.43 Å	−89.2	297.8	−287.5
r(F–F) = 1.34 Å	−126.8	431.4	−379.5
Δ	−37.6	133.6	−92.0

The observations in the previous paragraph apply equally well to the heavier X_2, and do not of themselves explain the long F_2 bond. Given that the Pauli term is the one which opposes shortening from r_{eqm}, we wondered if the rate of change of E^{Pauli} as the r(X–X) distance is reduced is greater for F_2 than for the other X_2 molecules. Fig. 4 shows that this is indeed the case. This figure plots E^{Pauli} for all four X_2 as a function of change in r(X–X) from equilibrium, and it is clear that the gradient in E^{Pauli} around r_{eqm} is steepest for F_2. We therefore suggest that the abnormally long (in the words of Caldow and Coulson) F_2 bond is a result of the high gradient of the E^{Pauli} curve, and hence the steepness of the inner wall of the potential well.

We can take this further and attempt an explanation for the relative gradients of the X_2 E^{Pauli} curves. Bickelhaupt and Baerends note that the kinetic energy component of E^{Pauli}, which is responsible for the overall destabilisation in the exchange repulsion as r(X–X) shortens, is strongly dependent upon the overlap of the orbitals on the separate fragments.[31] We have therefore summed all of the contributions to the S (overlap) matrix of the two X atoms for each X_2 as a function of internuclear separation, and the results are plotted on Fig. 4. It is quite clear that the change in X/X overlap as a function of r(X–X) is largest for F_2. Indeed, both the overlap and E^{Pauli} which depends on it are smallest for F_2 at $(r_{eqm} + 0.5)$ Å, but by $(r_{eqm} - 0.5)$ Å both overlap and E^{Pauli} are largest for F_2. Presumably this behaviour is a result of the compact nature of the F atom.

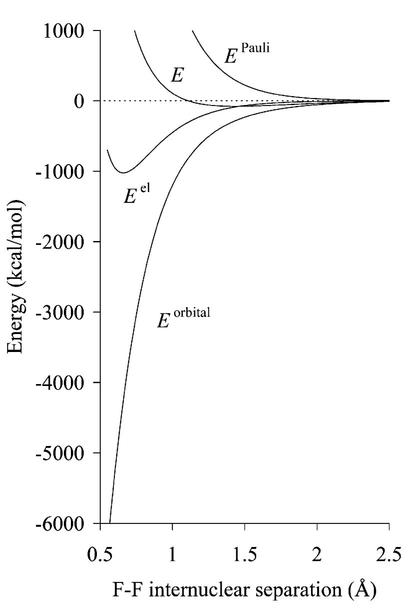

Fig. 3 Bond energy (kcal mol^{-1}) decomposition for F_2 as a function of r(F–F).

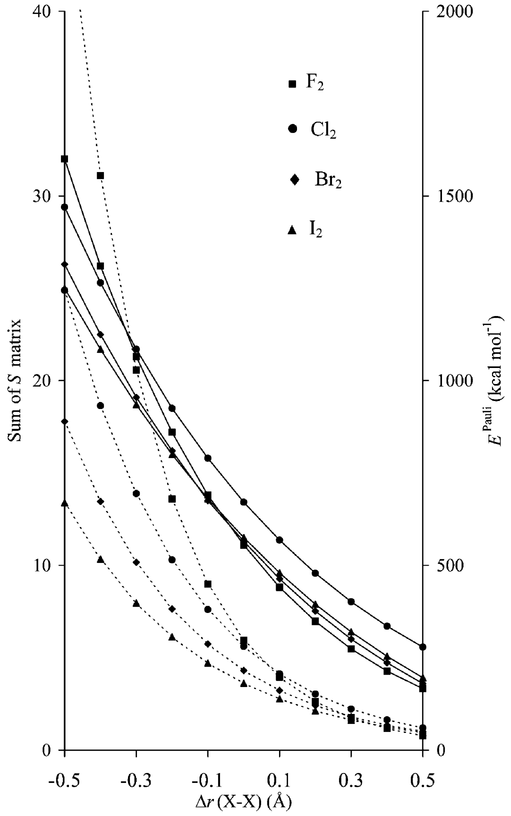

Fig. 4 Pauli repulsion (kcal mol^{-1}, dashed lines) and total X/X overlap (solid lines) for F_2, Cl_2, Br_2 and I_2 as a function of displacement from equilibrium geometry.

Conclusions

In this contribution we have used modern density functional methods to address the weakness of the F_2 bond. In particular we have probed the dependence on r(X–X) of the bond energy and its electrostatic, Pauli and orbital contributions using the Ziegler–Rauk scheme. Our main conclusions are as follows:

1. There is little evidence that d hybridisation plays a significant role.

2. At r_{eqm}, E^{Pauli} and $E^{orbital}$ display an approximately linear trend from $I_2 \rightarrow F_2$. By contrast, E^{el} for F_2 is some 30 kcal mol^{-1} less than would be expected on extrapolation of the $I_2 \rightarrow Cl_2$ trend. The weakness of the F_2 bond is therefore traced to a lower-than-expected E^{el} term, which we suggest arises from larger electron/electron repulsion at r_{eqm} for F_2 than for the heavier X_2.

3. The small E^{el} term for F_2 is a result of the unusually long F–F bond length. At r(F–F) = 0.1 Å shorter than r_{eqm} (the value expected on extrapolation of the differences between r(Se–Se) and r(Br–Br), and r(S–S) and r(Cl–Cl)) the E^{el} term is 37.6 kcal mol^{-1} more stabilising. There is clearly an electrostatic driving force toward a shorter r(F–F).

4. The long F–F bond is traced to the kinetic energy component of E^{Pauli}, which produces an overall destabilising change in E^{Pauli} around r_{eqm} which is significantly larger for F_2 than for the heavier X_2. The inner repulsive wall of the X_2 potential wells—a direct consequence of the Pauli repulsion—therefore occurs at relatively larger r(X–X) for F_2 than for the other X_2 molecules.

5. The greater change in E^{Pauli} as a function of r(X–X) for F_2 is a consequence of a comparatively larger change in X/X overlap with r(X–X) for F_2 than for the heavier halogens.

In summary, it is probably right to conclude, as do standard inorganic chemistry textbooks, that the weakness of the F_2 bond is a consequence of large electron/electron repulsion between the separate F atoms. However, this electrostatic repulsion only arises because of the behaviour of the Pauli repulsion. The weakness of the F_2 bond is therefore a quantum mechanically-driven electrostatic effect.

Note added in proof

We have recently become aware of a comparable study of F_2 by Esterhuysen and Frenking. This work will be published in a special issue of *Theoretical Chemistry Accounts*, dedicated to Jacopo Tomasi and due to appear at the start of 2004. We thank Professor Frenking for sharing this information with us.

Acknowledgements

We are grateful to University College London for a Teaching Assistantship to LEF, to the University of London's Central Research Fund and HEFCE/EPSRC (through the Joint Research Equipment Initiative) for computing equipment grants, and to the reviewers for their helpful comments.

References

1 K. P. Huber, G. Herzberg, *Molecular Spectra and Molecular Structure, IV. Constants of Diatomic Molecules*, Van Nostrand Reinhold, New York, 1979.
2 T. Ziegler and A. Rauk, *Theor. Chim. Acta.*, 1977, **46**, 1.
3 T. Ziegler and A. Rauk, *Inorg. Chem.*, 1979, **18**, 1558.
4 ADF2000 and 2002, *Department of Theoretical Chemistry*, Vrije Universiteit, Amsterdam.
5 E. J. Baerends, D. E. Ellis and P. Ros, *Chem. Phys.*, 1973, **2**, 41.
6 L. Versluis and T. Ziegler, *J. Chem. Phys.*, 1988, **88**, 322.
7 G. te Velde and E. J. Baerends, *J. Comp. Phys.*, 1992, **99**, 84.
8 C. Fonseca Guerra, J. G. Snijders, G. te Velde and E. J. Baerends, *Theor. Chem. Acc.*, 1998, **99**, 391.
9 N. Kaltsoyannis, *J. Chem. Soc., Dalton Trans.*, 1997, 1.
10 E. van Lenthe, R. van Leeuwen, E. J. Baerends and J. G. Snijders, *Int. J. Quantum Chem.*, 1996, **57**, 281.
11 E. van Lenthe, J. G. Snijders and E. J. Baerends, *J. Chem. Phys.*, 1996, **105**, 6505.
12 J. P. Perdew, J. A. Chevary, S. H. Vosko, K. A. Jackson, M. R. Pederson, D. J. Singh and C. Fiolhais, *Phys. Rev. B*, 1992, **46**, 6671.
13 J. P. Perdew, K. Burke and M. Ernzerhof, *Phys. Rev. Lett.*, 1996, **77**, 3865.
14 M. J. Frisch, G. W. Trucks, H. B. Schlegel, G. E. Scuseria, M. A. Robb, J. R. Cheeseman, V. G. Zakrzewski, J. A. Montgomery Jr., R. E. Stratmann, J. C. Burant, S. Dapprich, J. M. Millam, A. D. Daniels, K. N. Kudin, M. C. Strain, O. Farkas, J. Tomasi, V. Barone, M. Cossi, R. Cammi, B. Mennucci, C. Pomelli, C. Adamo, S. Clifford, J. Ochterski, G. A. Petersson, P. Y. Ayala, Q. Cui, K. Morokuma, D. K. Malick, A. D. Rabuck, K. Raghavachari, J. B. Foresman, J. Cioslowski, J. V. Ortiz, B. B. Stefanov, G. Liu, A. Liashenko, P. Piskorz, I. Komaromi, R. Gomperts, R. L. Martin, D. J. Fox, T. Keith, M. A. Al-Laham, C. Y. Peng, A. Nanayakkara, C. Gonzalez, M. Challacombe, P. M. W. Gill, B. Johnson, W. Chen, M. W. Wong, J. L. Andres, C. Gonzalez, M. Head-Gordon, E. S. Replogle and J. A. Pople, *Gaussian 98*, Gaussian Inc., 1998.
15 E. J. Baerends, V. Branchadell and M. Sodupe, *Chem. Phys. Lett.*, 1997, **265**, 481.
16 K. S. Pitzer, *J. Chem. Phys.*, 1955, **23**, 1735.
17 G. L. Caldow and C. A. Coulson, *Trans. Faraday Soc.*, 1962, **58**, 633.
18 R. S. Mulliken, *J. Am. Chem. Soc.*, 1955, **77**, 884.
19 L. Pauling, *The nature of the chemical bond*, Cornell University Press, Ithaca, NY, Third edn., 1960.
20 W. L. Jolly and C. J. Eyermann, *Inorg. Chem.*, 1983, **22**, 1566.
21 C. E. Housecroft, A. G. Sharpe, *Inorganic Chemistry*, Prentice Hall, Harlow, 2001.
22 D. F. Shriver, P. W. Atkins, *Inorganic Chemistry*, OUP, Oxford, Third edn., 1999.

23 J. Pittner, J. Smydke, P. Cársky and I. Hubac, *J. Mol. Struct. (Theochem)*, 2001, **547**, 239.

24 S. H. Vosko, L. Wilk and M. Nusair, *Can. J. Phys.*, 1980, **58**, 1200.

25 J. P. Perdew, S. Kurth, A. Zupan and P. Blaha, *Phys. Rev. Lett.*, 1999, **82**, 2544.

26 F. Moscardó, A. J. Pérez-Jiménez and J. A. Cjuno, *J. Comp. Chem.*, 1998, **19**, 1899.

27 W. Koch, M. C. Holthausen, *A Chemist's Guide to Density Functional Theory*, Wiley-VCH, Weinheim, Second edn., 2001.

28 S. X. Xiao, W. C. Trogler, D. E. Ellis and Z. Berkovitch-Yellin, *J. Am. Chem. Soc.*, 1983, **105**, 7033.

29 D. L. Cooper, T. P. Cunningham, J. Gerratt, P. B. Karadakov and M. Raimondi, *J. Am. Chem. Soc.*, 1994, **116**, 4414.

30 N. Kaltsoyannis, *J. Chem. Soc., Dalton Trans.*, 1997, 4759.

31 F. M. Bickelhaupt and E. J. Baerends, in *Reviews in Computational Chemistry*, eds. K. B. Lipkowitz and D. B. Boyd, Wiley-VCH, New York, 2000, vol. 15, pp. 1.

32 K. A. Peterson, R. A. Kendall and T. H. Dunning, *J. Chem. Phys.*, 1993, **99**, 9790.

33 L. A. Curtiss, P. C. Redfern, B. J. Smith and L. Radom, *J. Chem. Phys.*, 1996, **104**, 5148.

34 P. C. Redfern, J.-P. Blaudeau and L. A. Curtiss, *J. Phys. Chem. A*, 1997, **101**, 8701.

35 A. G. Császár and W. D. Allen, *J. Chem. Phys.*, 1996, **104**, 2746.

36 J. M. L. Martin and O. Uzan, *Chem. Phys. Lett.*, 1998, **282**, 16.

37 P. C. Hiberty, J. P. Flament and E. Noizet, *Chem. Phys. Lett.*, 1992, **189**, 259.

38 M. Filatov and W. Thiel, *Phys. Rev. A*, 1998, **57**, 189.